STRENGTH AND DUCTILITY OF REINFORCED AND PRESTRESSED CONCRETE COLUMNS AND PILES UNDER SEISMIC LOADING

R. Park (I)
F.A. Zahn (II)
T.J. Falconer (III)
Presenting Author: R. Park

SUMMARY

The results of recent experimental and analytical studies of the strength and ductility of a range of reinforced concrete columns and prestressed concrete piles when subjected to severe earthquake loading are summarized. The column and pile units had a 400 mm square or octagonal cross section. The transverse reinforcement was from either Grade 275 or 380 steel. The units were loaded axially and by cyclic lateral loading at mid-height along either a section diagonal or principal axis to various displacement ductility levels. The units with transverse reinforcement designed according to the New Zealand Code showed stable lateral load-deflection hysteresis loops up to a displacement ductility factor of at least six.

INTRODUCTION

The need in seismic design to detail structural concrete compression members with sufficient transverse reinforcement to ensure ductile behaviour is recognised by codes. An earlier paper (Ref. 1) reported the results of some tests on reinforced concrete columns which contained transverse reinforcement close to the quantity required in potential plastic hinge regions by the New Zealand Concrete Design Code (Ref. 2). The present paper summarizes investigations of the strength and ductility of a further range of reinforced concrete columns and prestressed concrete piles with transverse reinforcement designed using the provisions of that code.

NEW ZEALAND CONCRETE DESIGN CODE PROVISIONS

According to the New Zealand Code (Ref. 2) the potential plastic hinge region should be considered to extend over the end length of column not less than the larger of the column diameter in the case of a circular column or the longer column cross section dimension in the case of a rectangular column, or where the moment exceeds 0.8 of the maximum moment at that end of the member. An exception is that when $P_e > \phi 0.3 f'_c A_g$ the above length should be increased by 50%. In the potential plastic hinge region the maximum centre to centre spacing of the transverse reinforcement should not exceed the smaller of one-fifth of the column diameter or one-fifth of the smaller column cross section dimension, or six longitudinal bar diameters, or 200 mm. When spirals or circular hoops are used, ρ_s should not be less than the greater of

(I) Professor of Civil Engineering, University of Canterbury, New Zealand.

(II) Graduate Student, Department of Civil Engineering, University of Canterbury, New Zealand.

(III) Design Engineer, Payne, Sewell and Partners, Wanganui, New Zealand.

$$\rho_s = 0.45\left(\frac{A_g}{A_c} - 1\right)\frac{f'_c}{f_{yh}}\left(0.5 + 1.25\frac{P_e}{\phi f'_c A_g}\right) \tag{1}$$

$$\text{or } \rho_s = 0.12\,\frac{f'_c}{f_{yh}}\left(0.5 + 1.25\frac{P_e}{\phi f'_c A_g}\right) \tag{2}$$

where P_e should be less than either $\phi 0.7 f'_c A_g$ or $\phi 0.7 P_o$. When rectangular hoops with or without supplementary cross ties are used, the total area of hoop bars and supplementary cross ties in each of the principal directions of the cross section within spacing s_h should be not less than the greater of

$$A_{sh} = 0.3 s_h h''\left(\frac{A_g}{A_c} - 1\right)\frac{f'_c}{f_{yh}}\left(0.5 + 1.25\frac{P_e}{\phi f'_c A_g}\right) \tag{3}$$

$$\text{or } A_{sh} = 0.12 s_h h''\,\frac{f'_c}{f_{yh}}\left(0.5 + 1.25\frac{P_e}{\phi f'_c A_g}\right) \tag{4}$$

where P_e should be less than either $\phi 0.7 f'_c A_g$ or $\phi 0.7 P_o$. The centre to centre spacing across the section between cross linked bars should not exceed 200 mm where rectangular hoops are used.

Eqs. 1 to 4 are based on the SEAOC (Ref. 3) recommendations modified to take into account the effect of axial load level. The modification was based on the results of moment-curvature analyses conducted using idealised stress-strain curves for confined concrete (see for example Refs. 4 and 5) and from column test results (see for example Ref. 1). The greater confinement at higher axial load is necessary because of the greater depth of compressed concrete, and hence the greater dependence on the concrete.

TESTS ON COLUMNS WITH CONCENTRIC COMPRESSIVE LOADING

The quantity of transverse steel required by Eqs. 1 to 4 is dependent partly on the yield strength of the steel. To check this assumption for two grades of New Zealand steel, three pairs of concentrically loaded spirally reinforced concrete column units of the dimensions shown in Fig. 1a were tested. In each pair the spiral reinforcement was from 12 mm diameter Grade 275 bar in one column unit and from 10 mm diameter Grade 380 bar in the other unit, so that the yield force of the spiral bar $A_{sp} f_{yh}$ was approximately the same for both units in the pair. Four linear potentiometers, mounted on steel rods embedded in the concrete as shown in Fig. 1a, were used to measure the longitudinal strain over a 500 mm gauge length. A 10 MN capacity DARTEC testing machine was used to apply the load monotonically at a slow uniform strain rate until fracture of the spiral bar occurred. Fig. 1b shows the load-strain curves measured for the pair of column units with a spiral pitch of 75 mm and ρ_s = 1.61% for the Grade 275 spiral and 1.12% for the Grade 380 spiral. The similarity between the two load-strain curves in Fig. 1b, and the fact that the longitudinal strain when the spiral fractures is not particularly different for the two columns, justifies the use of smaller quantities of high strength steel. The comparison between the load-strain curves of the other two pairs of columns, with spiral pitches of 40 mm and 135 mm, led to a similar conclusion. It is to be noted that the stage of first fracture of the transverse reinforcement can be regarded as the end of the useful region of the stress-strain curve for the confined concrete core, since the concrete is then no longer effectively confined (Ref. 6). The stress-strain curves for the reinforcement used for the spirals indicated that the strain when strain hardening commenced and when fracture occurred was 2.5% and 24% respectively for the Grade 275 steel, and 1.65% and 18% respectively for the Grade 380 steel. It is evident that the effect of the earlier and greater strain hardening of the higher strength steel, and hence greater potential to store strain energy, offset the effect of the lower fracture strain of that steel.

TESTS ON COLUMNS AND PILES WITH CYCLIC LATERAL LOADING

Column and Pile Test Units

Fig. 2 and Tables 1 and 2 give the details of the units. The quantities of transverse reinforcement present in the units, as a percentage of that required by Eqs. 1 to 4 for the actual material strengths and column load levels imposed, are also shown in Tables 1 and 2. Pile Unit 4 was deliberately designed to have a small quantity of spiral reinforcement. The spacing of transverse reinforcement satisfied the requirements of Ref. 2, except that in Column Units 5 and 7 the spacing exceeded the $6d_b$ limitation by 41% and 22%, respectively.

Fig. 3 shows the loading arrangements and principal dimensions of the column and pile test units. Each unit had a reinforced concrete stub at mid-height which simulated a beam or pier cap. The axial column compressive load P_e was held constant during each test using a 10 MN capacity DARTEC machine to the values of P_e/f'_cA_g listed in Tables 1 and 2. The reversible horizontal load at the stub was applied by a 500 kN MTS actuator. In the case of the square column units the horizontal load was applied in the direction of the diagonal of the section if indicated by the ◇ symbol in Table 1, or in the direction of a principal axis of the section if indicated by the □ symbol. The horizontal load was cycled at a slow rate in a displacement controlled pattern. Two complete cycles each to displacement ductility factors Δ/Δ_y of ±2, ±4, ±6, ... were applied. The first yield displacement Δ_y was taken to be the calculated displacement when the critical section reached moment M_y assuming that the unit behaved elastically up to that moment with constant flexural rigidity equal to that found at $0.75M_y$, where for the column units M_y was taken as the measured moment at first crushing of the cover concrete and for the pile units M_y was taken as the theoretical flexural strength calculated by the ACI code method (Ref. 7) using the actual material strengths and $\phi = 1$.

Results from Reinforced Concrete Columns and Prestressed Concrete Piles

Fig. 4a,b,c,d and e show typical measured horizontal load-displacement hysteresis loops. The measured loops, with the exception of that for Pile Unit 4, illustrate very good stable behaviour with limited strength degradation. This good behaviour was also demonstrated by the loops of the other units. The square columns loaded along the section diagonal proved to be more ductile than those loaded along a principal axis of the section. For the square columns the two arrangements of overlapping hoops used were equally effective (Fig. 2a and b). Yielding of transverse reinforcement (hoops and spirals) in all units occurred during the testing. Generally this yielding commenced at a lower displacement ductility factor for the units with large axial load than for the units with small axial load. The confining action was adequately maintained during the testing, except for Pile Unit 4. The columns confined by Grade 380 steel behaved as adequately as those confined with Grade 275 steel. Column Units 5 and 7 which had hoop spacing in excess of $6d_b$ showed extensive buckling of longitudinal bars once displacement ductility factors of 6 were reached.

The concrete longitudinal compressive strains measured when crushing of cover concrete first became visible, and the maximum compressive strains measured on the surface of the confined concrete core, are listed in Tables 3 and 4. These strains were calculated from deformations measured over a gauge length of up to 150 mm by linear potentiometers or dial gauges placed between steel rods which passed through the units in the plastic hinge regions.

The plastic rotation commenced either above or below the central stub in most of the units. This situation is illustrated in Fig. 5, where θ is the stub rotation. To find the true horizontal displacement of each half length of column the quantity θh has to be added to or subtracted from the horizontal displacement at the stub Δ. The maximum displacement ductility factors reached when the measured moment capacities had not reduced to less than 0.9 of the maximum measured moments are shown in Table 3 for the reinforced concrete column units. The footnote to Table 4 gives an indication of the displacement ductility values reached using a similar criterion for the prestressed concrete pile units.

The theoretical flexural strengths M_{aci} of the sections of the units calculated by the ACI method (Ref. 7) using the actual material strengths and assuming $\phi = 1$ are shown in Tables 3 and 4. The measured maximum moments exceeded the ACI theoretical values by a wide margin, particularly for the diagonally loaded units and for the well confined units with high axial load. The theoretical ultimate horizontal load calculated using these ACI moments and allowing for the P-Δ effect are also shown plotted in Fig. 4.

A refined moment-curvature analysis for monotonic flexure was conducted taking into account the enhanced strength and ductility of confined concrete using analytical stress-strain curves(from Refs. 6 and 8 for the reinforced concrete column units and from Ref. 5 for the prestressed concrete pile units) and the measured stress-strain curves for the steel. As indicated in Tables 3 and 4 the maximum moments M_{calc} given by these theoretical predictions proved to be conservative, no doubt due to the higher stresses reached by reinforcing steel when loaded cyclically with inelastic strains in both the tension and compressive ranges, and due to the additional confinement from the stiff central stub which would shift the critical section away from the face of the stub. Fig. 6 shows the theoretical moment-curvature relations for Column Unit 2 loaded diagonally and also for the same section if it were loaded uniaxially. The tests and theory indicated similarly ductile behaviour for both uniaxial and biaxial bending and hence no special precautions need to be taken for the biaxial loading case if ductile detailing for the uniaxial loading case is provided.

CONCLUSIONS

The quantity of transverse steel recommended by the New Zealand Code in potential plastic hinge zones resulted in displacement ductility factors greater than 6 being achieved by the reinforced concrete columns and prestressed concrete piles during cyclic loading with only a small degradation of strength.

REFERENCES

1. R. Park, M.J.N. Priestley, W.D. Gill, R.T. Potangaroa, "Ductility and Strength of Reinforced Concrete Columns With Spirals or Hoops Under Seismic Loading", Proceedings of 7th World Conference on Earthquake Engineering, Vol. 7, Istanbul, September 1980.
2. Standards Association of New Zealand, "Code of Practice for the Design of Concrete Structures", NZS 3101, Parts 1 and 2, Wellington, 1982.
3. Structural Engineers Association of California Seismology Committee, "Recommended Lateral Force Requirements and Commentary", San Francisco, 1975.
4. R. Park and T. Paulay, "Reinforced Concrete Structures", John Wiley and Sons, New York, 1975.
5. R. Park and P.D. Leslie, "Curvature Ductility of Circular Reinforced Concrete Columns Confined by the ACI Spiral", 6th Australasian Conference on the Mechanics of Structures and Materials, Vol. 1 : Technical Papers, Christchurch, New Zealand, August 1977.
6. B.D. Scott, R. Park and M.J.N. Priestley, "Stress-Strain Behaviour of Concrete Confined by Overlapping Hoops at Low and High Strain Rates", Journal of American Concrete Institute, Proc. V.79, No. 1, Jan-Feb. 1982.
7. American Concrete Institute, "Building Code Requirements for Reinforced Concrete, ACI 318, Detroit, 1977.
8. S.P. Shah and A. Fafitis, "Cyclic Loading of Spirally Reinforced Concrete", Journal of Structural Engineering, American Society of Civil Engineers, Vol. 109, No. 7, July 1983.

NOTATION

A_c = area of concrete core measured to outside of spiral or hoop
A_g = gross area of column section
A_{sh} = total effective area of hoop bars at spacing s_h
A_{sp} = area of spiral bar
d_b = bar diameter
f'_c = compressive cylinder strength of concrete
f_{pu} = tensile strength of prestressing steel
f_y = yield strength of longitudinal reinforcing steel
h = one-half height of column specimen
h'' = width of concrete core, perpendicular to the direction of hoop legs
M_{aci} = flexural strength calculated by ACI code method
M_{calc} = maximum theoretical moment calculated from moment-curvature analysis
M_{exp} = maximum moment measured in tests
P_e = maximum design compressive load due to gravity and seismic loading
P_o = axial load strength when load is applied with zero eccentricity
s_h = centre to centre spacing of spiral or hoop sets
ε_{cu} = strain at extreme compression fibre of concrete
θ = rotation of central stub
ϕ = strength reduction factor equal to 1.0 if the column design actions are such as to provide a high degree of protection against plastic hinging of columns, otherwise equal to 0.9
ρ_s = ratio of volume of spiral or hoop reinforcement, including supplementary cross ties, if any, to volume of concrete core
ρ_t = ratio of area of longitudinal reinforcement or prestressing strand to A_g
Δ = maximum lateral displacement
Δ_y = lateral displacement at first yield

Column Units	Cross Section	f'_c [a] MPa	$\frac{P_e}{f'_c A_g}$	Longitudinal Reinforcement Dia. mm	Longitudinal Reinforcement f_y MPa	Longitudinal Reinforcement ρ_t %	Transverse Reinforcement[b] Dia. mm	Transverse Reinforcement[b] f_{yh} MPa	Transverse Reinforcement[b] s_h mm	Transverse Reinforcement[b] ρ_s %	Transverse Reinforcement[b] $\frac{\rho_s \text{ provided}}{\rho_s \text{ NZS 3101}}$[c]
1	◇ Fig. 2b	31.6	0.27	16	423	1.51	10	318	84	2.24	1.00
2	◇ Fig. 2b	28.0	0.45	16	423	1.51	10	318	65	2.89	1.15
3	◇ Fig. 2a	32.1	0.23	16	423	1.51	10	318	72	2.14	1.04
4	◇ Fig. 2a	23.5	0.48	16	423	1.51	10	318	55	2.80	1.34
5	○ Fig. 2c	32.1	0.13	16	337	2.43	10	466	135	0.61	1.11
6	○ Fig. 2c	23.5	0.67	16	337	2.43	10	466	75	1.09	1.35
7	□ Fig. 2b	28.0	0.23	16	440	1.51	10	466	117	1.56	1.26
8	□ Fig. 2b	37.2	0.42	16	440	1.51	10	466	92	1.99	0.93

a. At time of testing units
b. Over length of potential plastic hinge region of 400 mm for Units 1, 3, 5 and 7, and 600 mm for Units 2, 4, 6 and 8. Spacing of transverse reinforcement was increased outside these regions.
c. Using measured steel and concrete strengths and $\phi = 1$.

Table 1
Details of Reinforced Concrete Column Units

Pile Unit[a]	f'_c [b] MPa	$\frac{P_e}{f'_c A_g}$	Longitudinal Prestressing Strand[c] Dia. mm	Longitudinal Prestressing Strand[c] f_{pu} MPa	Longitudinal Prestressing Strand[c] ρ_t %	Longitudinal Nonprestressed Reinforcement Dia. mm	Longitudinal Nonprestressed Reinforcement f_y MPa	Longitudinal Nonprestressed Reinforcement ρ_t %	Spiral Reinforcement[d] Dia. mm	Spiral Reinforcement[d] f_{yh} MPa	Spiral Reinforcement[d] s_h mm	Spiral Reinforcement[d] ρ_s %	Spiral Reinforcement[d] $\frac{\rho_s \text{ provided}}{\rho_s \text{ NZS3101}}$[e]
1	37.0	0.3	12.5	1824	0.73	20	292	2.37	10	284	35	2.64	1.12
2	38.7	0.3	12.5	1824	0.73	-	-	-	10	284	35	2.64	1.08
3	42.7	0.1	12.5	1824	0.73	-	-	-	10	284	45	2.05	1.06
4	33.6	0.3	12.5	1824	0.73	-	-	-	10	284	130	0.71	0.33
5	29.2	0.6	12.5	1824	0.73	-	-	-	12	318	35	3.80	1.62

a. Section as shown in Fig. 2d
b. At time of testing units
c. The estimated stress in the prestressing steel at time of testing was $0.64f_{pu}$ giving a prestress in the concrete of 8.54 MPa
d. Over length of potential plastic hinge region of 400 mm for Unit 1, 2, 3 and 4, and 600 mm for Unit 5. Spacing of the spirals was increased outside these regions
e. Using measured steel and concrete strengths and $\phi = 1$.

Table 2
Details of Prestressed Concrete Pile Units

Column Unit	Experimental Concrete Compression Strain ε_{cu}: First Visible Crushing	Experimental Concrete Compression Strain ε_{cu}: Maximum Measured Value	Displacement Ductility Factor When Moment Capacity Had Not Reduced to $< 0.9 M_{exp}$: $\frac{\Delta}{\Delta_y}$	Displacement Ductility Factor When Moment Capacity Had Not Reduced to $< 0.9 M_{exp}$: $\frac{\Delta + \theta h}{\Delta_y}$	Flexural Strength: M_{exp} kNm	Flexural Strength: ACI Code Method M_{aci}[a] kNm	Flexural Strength: ACI Code Method M_{exp}/M_{aci}	Flexural Strength: Refined Moment-Curvature Analysis M_{calc}[b] kNm	Flexural Strength: Refined Moment-Curvature Analysis M_{exp}/M_{calc}
1	0.005	0.050	>10.3	>15.4	368	273	1.35	299	1.23
2	0.007	0.041	> 9.5	>11.1	400	259	1.54	309	1.29
3	0.006	0.044	>10.3	>10.9	357	273	1.31	292	1.22
4	0.0055	0.047	>12.5	>13.0	397	234	1.70	285	1.39
5	0.0055	0.045	6.9	9.6	234	217	1.08	220	1.06
6	0.005	0.055	6.6	12.8	325	193	1.68	237	1.37
7	0.0075	0.035	6.1	7.4	335	284	1.18	299	1.12
8	0.008	0.040	7.0	9.5	433	352	1.23	408	1.06
							Average = 1.38		Average = 1.22

a. Flexural strength obtained from ACI code method using actual material strengths and assuming $\phi = 1$
b. Maximum moment attained in theoretical moment-curvature relation.

Table 3
Experimental and Theoretical Results for Reinforced Concrete Column Units

Pile Unit	Experimental Concrete Compression Strain ε_{cu}: First Visible Crushing	Experimental Concrete Compression Strain ε_{cu}: Maximum Measured Value	Flexural Strength: M_{exp} kNm	Flexural Strength: ACI Code Method M_{aci}[a] kNm	Flexural Strength: ACI Code Method M_{exp}/M_{aci}	Flexural Strength: Refined Moment-Curvature Analysis M_{calc}[b] kNm	Flexural Strength: Refined Moment-Curvature Analysis M_{exp}/M_{calc}
1	0.005	0.063	429	294	1.46	371	1.16
2	0.005	0.128	320	252	1.27	284	1.13
3	0.005	0.054	275	231	1.19	253	1.09
4	0.005	0.081	255	209	1.22	221	1.05
5	0.005	0.135	294	123	2.39	284	1.04
					Average = 1.51		Average = 1.09

a. Flexural strength obtained from ACI code method using actual material strengths and assuming $\phi = 1$.
b. Maximum moment attained in theoretical moment-curvature relation.
c. Δ/Δ_y was generally rather greater than 6 when the measured moment had not reduced to $< 0.9M_{exp}$, except for Unit 4 where the measured moment decreased abruptly when Δ/Δ_y exceeded 2.

Table 4
Experimental and Theoretical Results for Prestressed Concrete Pile Units

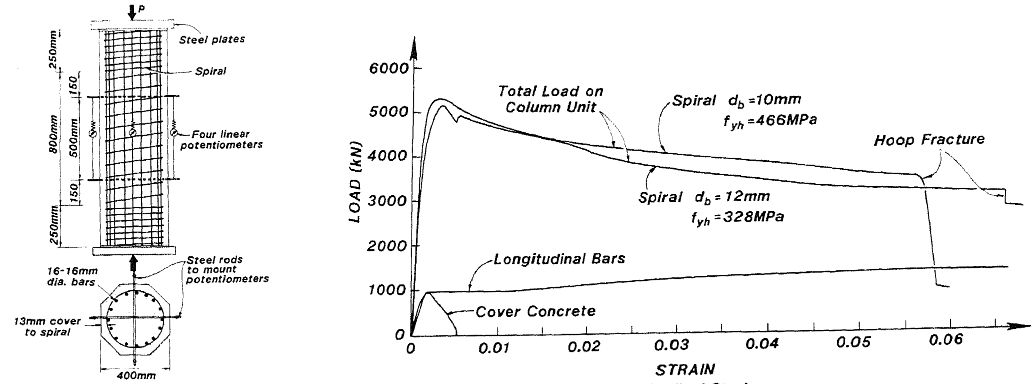

(a) Principal Dimensions and Test Set Up

(b) Measured Load Versus Longitudinal Strain

Fig. 1 Measured Results from Concentric Monotonic Compression Tests.

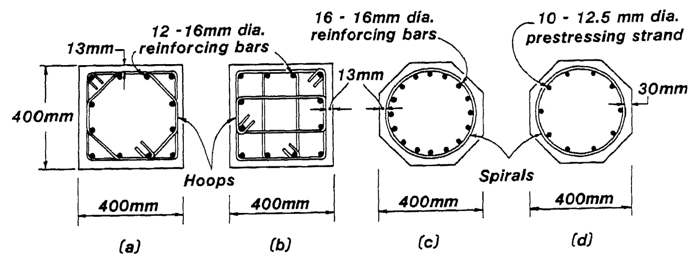

Fig. 2 Cross Sections of Columns and Piles.

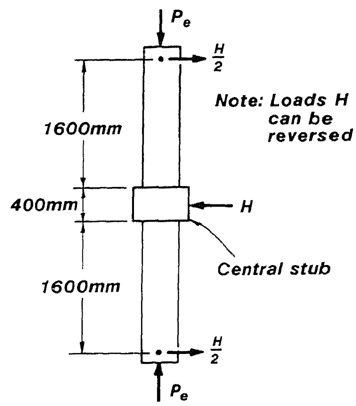

Fig. 3 Loading Arrangements.

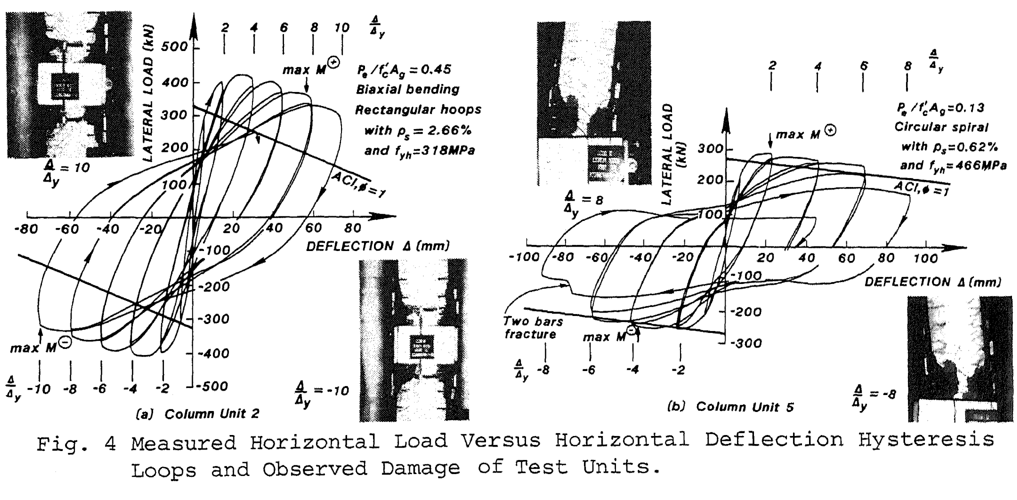

Fig. 4 Measured Horizontal Load Versus Horizontal Deflection Hysteresis Loops and Observed Damage of Test Units.

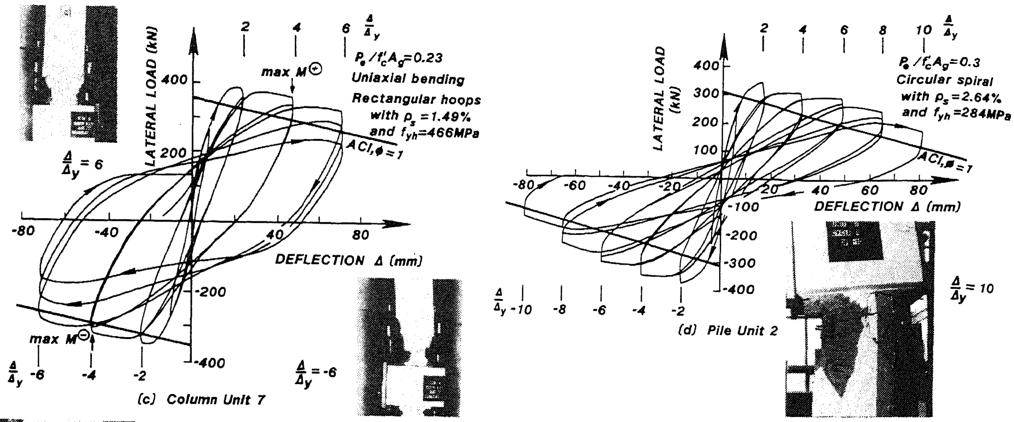

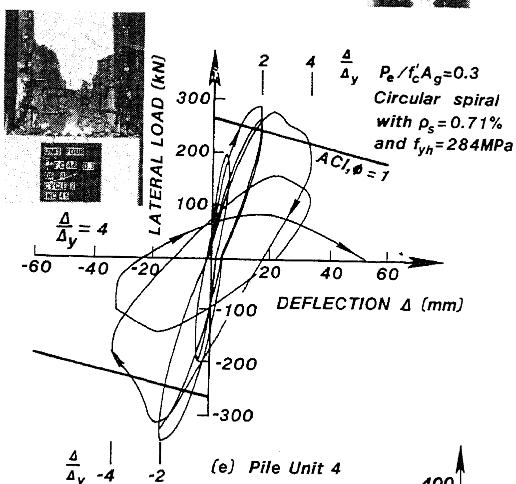

Fig. 4 Measured Horizontal Load Versus Horizontal Deflection Hysteresis Loops and Observed Damage of Test Units (Continued)

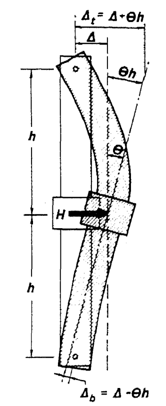

Fig. 5 Implication of Rotation of Central Stub of Test Units.

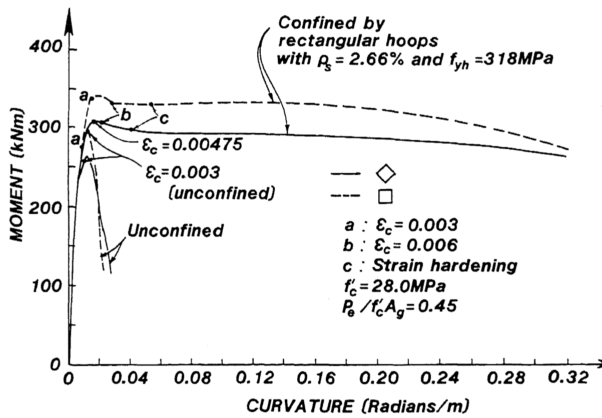

Fig. 6 Theoretical Moment-Curvature Relations for Section of Column Unit 2 Loaded Diagonally and Also for the Same Section if it Were Loaded Uniaxially.